THE JOURNAL OF PHYSICAL CHEMISTRY B

B: Biophysics; Physical Chemistry of Biological Systems and Biomolecules

Intrinsic Antioxidant Potential of the Aminoindole Structure. A Computational Kinetics Study of Tryptamine

Erika N. Bentz, Rosana Maria Lobayan, Henar Martinez, Pilar Redondo, and Antonio Largo

J. Phys. Chem. B, **Just Accepted Manuscript** • DOI: 10.1021/acs.jpcb.8b03807 • Publication Date (Web): 18 May 2018

Intrinsic Antioxidant Potential of the Aminoindole Structure. A Computational Kinetics Study of Tryptamine

Erika N. Bentz,[a] Rosana M. Lobayan,[a,*] Henar Martínez,[b] Pilar Redondo,[c] Antonio Largo[c,*]

[a] *Departamento de Física, Facultad de Ciencias Exactas y Naturales y Agrimensura, Universidad Nacional del Nordeste, Avda. libertad 5300, 3400 Corrientes, Argentina.*
[b] *Departamento de Química Orgánica, Escuela de Ingenierías Industriales, Universidad de Valladolid, Campus Esgueva, Paseo del Cauce 59, 47011 Valladolid, Spain.*
[c] *Departamento de Química Física y Química Inorgánica, Facultad de Ciencias, Universidad de Valladolid, Campus Miguel Delibes, Paseo de Belén 7, 47011 Valladolid, Spain.*
*Corresponding authors: rlobayan@unne.edu.ar; alargo@qf.uva.es
Electronic Supplementary Information (ESI) available: The RAF products for the reaction of TRA with $HOO^{\bullet}$ radical are given in Figure S1.

Abstract

A computational kinetics study of the antioxidant activity of tryptamine toward $HO^{\bullet}$ and $HOO^{\bullet}$ radicals in water at 298 K has been carried out. Density functional methods have been employed for the quantum chemical calculations and conventional transition state theory was used for rate constants evaluation. Different mechanisms have been considered: radical adduct formation (RAF), single electron transfer (SET), and hydrogen atom transfer (HAT). For the reaction of tryptamine with the hydroxyl radical nearly all channels are diffusion controlled, and the overall rate constant is very high, 6.29×10^{10} M^{-1} s^{-1}.The RAF mechanism has a branching ratio of 55%, followed by the HAT mechanism (31%), whereas the SET mechanism accounts just for 13% of the products. The less hindered carbon atom neighbor to the nitrogen of the indole ring seems to be the preferred site for the RAF mechanism, with a branching ratio of 16%. The overall rate constant for the reaction of tryptamine with the $HOO^{\bullet}$ radical is 3.71×10^{4} M^{-1} s^{-1}, suggesting that it could be a competitive process with other reactions of hydroperoxyl radicals in biological environments. For this reaction only the HAT mechanism seems viable. Furthermore, only two centers may contribute to the HAT mechanism, the nitrogen atom of the indole ring and a carbon atom of the aminoethyl chain, the former accounting for more than 91% of the total products. Our results suggest that tryptamine could have a noticeable scavenging activity toward radicals, and that this activity is mainly related to the nitrogen atom of the indole ring thus showing the relevance of their behavior in the study of aminoindoles.

Introduction

Tryptamine (TRA) is a neurotransmitter closely related to the amino acid tryptophan. In fact, both molecules share the indole ring and the aminoethyl side-chain. The difference resides in the carboxylic group at the end of the chain present in tryptophan. Other related molecules with important biological activity are the neurotransmitter serotonin (5-hydroxytryptamine) and the neurohormone melatonin (5-methoxy-N-acetyltriptamine). Several other substituted tryptamines play also a role as neurotransmitters or drugs.

In addition to its biological activity related to the nervous system, tryptamine and derived compounds have a remarkable antioxidant activity. Oxidative stress has undesirable effects on living beings since it is related to several health diseases and degenerative disorders. Oxidative stress is caused by the effect of free radicals on living organisms. Therefore, antioxidants that can avoid or ameliorate the damage caused by free radicals are highly valuable. Different types of antioxidant activity can be identified: enzyme inhibitors, metal chelators, or radical scavengers.[1] TRA, as well as other compounds having an indole ring, seems to have antioxidant properties as radical scavengers.[2,3]

Several experimental studies[4-7]have been conducted to study the antioxidant activity of substituted tryptamines, particularly melatonin (MLT). From the theoretical side, different studies have tried to ascertain the possible mechanisms operating in the antioxidant activity of melatonin and related compounds.[8-13]

All indolamines share an heteroaromatic ring of high electronegativity and they only differ in several substitutions and groups in their side chain. The experimental results indicated that the scavenging of free radicals by indole compounds depends on the presence of the indole ring, and also of their functional residues which modulated the reactivity of these molecules.[15] In fact, the presence of different substituents affects the antioxidant activity of indolamines, but TRA is especially relevant since it possess the essential skeleton of this type of molecules. Therefore, it would be interesting to know the role of the different possible mechanisms in the antioxidant activity of TRA, since this would provide information about the intrinsic antioxidant potential of the aminoindole structure common to different potentially interesting molecules with antioxidant activity. This is precisely the main purpose of the present work.

The conformers of TRA have been studied in detail in the gas phase through different experimental techniques.[16-20] The results obtained through theoretical analysis[21] are basically in agreement with the experimental observations. The analysis of the conformational space of TRA were further extended by theoretical studies considering solvent effects.[22] Moreover, a

recent paper showed[23] the significance of the knowledge of electronic distribution of TRA and its behavior to understand the values of thermodynamic parameters necessary for the study of the free radical scavenging capacity. More precisely, the quantification of the changes measured in serotonin (5-hydroxytryptamine, SER) regarding TRA as reference allowed concluding that the variations on the electronic population at the nitrogen belonging of the indole ring, and the electronic delocalizations from that site and those related to the π-electronic system, enabled us to explain variations associated with free radical scavenging capacity. To apply new hypotheses, it is therefore of interest to deepen the knowledge of the role of indole ring, in TRA as a model of aminoindol structures, which as already shown is significant in the antioxidant activity, through the kinetics study. Since the study of the antioxidant activity of TRA should approach as much as possible the conditions in living organisms, it is desirable to carry out simulations in a solvent environment. For that reason, we will adopt in our work the predicted conformational structure in theoretical simulations in aqueous solution.[22]

Our purpose is to analyze the antioxidant properties of TRA. As model oxidant agents, we have taken into account the hydroxyl ($HO^{\bullet}$) and hydroperoxyl ($HOO^{\bullet}$) radicals. Despite their apparently close structure, these radicals behave in a rather different way. Hydroxyl is very reactive, with a half-life in the scale of nanoseconds. On the other hand, hydroperoxyl is less reactive and has a half-live in the scale of seconds.[21] In addition, HOO· is a good model to understand the behavior of larger peroxyl radicals. The importance of analyzing the kinetics of the mechanisms to scavenge HO● radicals was previously recognized considering that the protective effect against lipid peroxidation does not occur directly trapping peroxyl radicals, but by the capture of more reactive radicals such as HO●, which are fundamental since these radicals would be the ones that initiate the process of degradation.[10]

Previous studies of Molecular Electrostatic Potential for parent molecule also will be helpful to analyze some obtained results.[22]

Computational methods

We have adopted a computational methodology that has been successfully applied and tested in many other studies.[10-13,25-29] Galano and Alvarez-Idaboy[30] paved the way for the design of a computational strategy for the accurate prediction of rate constants in solution, which can be applied to evaluate the antioxidant activity of chemical compounds. They termed this methodology QM-ORSA (quantum mechanics-based overall free radical scavenging activity).[30] A detailed account of this methodology can be found in ref. 30. We will just summarize the main points.

Geometry optimizations of all species were carried out using the M05-2X functional,[31] which has been parameterized for kinetic calculations, in conjunction with the 6-311++G(d,p) basis set.[32] The *Gaussian 09* program[33] was employed in all electronic structure calculations. For all open-shell species unrestricted calculations were performed. Harmonic vibrational calculations were carried out at the optimized geometries. In such way the nature of stationary points can be determined (all frequencies real for minima and one imaginary frequency for transition states). In addition, frequency calculations allow an estimate of the zero-point energy correction to the electronic energies. Thermal corrections to the energies (at 298 K) were also included.

A continuum model has been employed for mimicking solvent effects. In particular the SMD model[34] was chosen, in part due to the employment of the M05-2X functional in the parameterization of the SMD model. Solvent cage effects, taking into account the free volume theory, are incorporated following the corrections proposed by Okuno[35]. In addition, the 1M standard state in solution must be incorporated, as opposite to the 1atm standard state operating in the gas phase. This correction due to the standard state is particularly relevant when computing rate constants for bimolecular processes since the energy barriers are affected.[30]

The rate constants are calculated using conventional transition state theory (TST) through the standard formula:

$$k = \sigma\,\tau\,\frac{k_B}{h}e^{-(\Delta G^{\neq})/RT} \qquad (1)$$

Where σ corresponds to the reaction path degeneracy, τ is the tunneling correction, and k_B and h are the Boltzmann and Planck constants, respectively. For the estimation of tunneling corrections we have employed the zero-curvature tunneling method[36] employing an Eckart barrier.

For those reactions where a transition state cannot be located using electronic structure methods, such as for single electron-transfer (SET) processes, Marcus theory[37,38] will be employed. In those cases the energy barrier is estimated as

$$\Delta G^{\neq} = \frac{\lambda}{4}\left(1 + \frac{\Delta G^{o}}{\lambda}\right)^{2} \qquad (2)$$

employing two thermodynamic parameters, the nuclear reorganization energy (λ) and the free energy of reaction (ΔG^{o}). A simple approach to λ is given by:

$$\lambda = \Delta E - \Delta G^o \qquad (3)$$

where ΔE is the vertical energy difference between reactants and products for the electron transfer process. A similar procedure has been previously applied in a number of reactions.[39,40]

Since we are dealing with reactions in solution, diffusion may play a crucial role. For very fast processes the limiting factor could be the diffusion rate. In order to obtain the apparent rate constant for any channel considered in the global process, we will follow the suggestion of Galano and Alvarez-Idaboy.[30] These authors propose to employ the Collins-Kimball theory to obtain the apparent rate constant

$$k_{app} = \frac{k_D\, k}{k_D + k} \qquad (4)$$

in terms of the thermal rate constant (k) and the steady-state Smoluchowski rate constant (k_D). The latter is obtained as

$$k_D = 4\,\pi\, R_{AB} D_{AB} N_A \qquad (5)$$

where R_{AB} is the reaction distance, D_{AB} is the mutual diffusion coefficient, and N_A the Avogadro number.D_{AB} is computed employing the reactants diffusion coefficients,[41] and these are calculated through the well-known Stokes-Einstein formula:

$$D_A = \frac{k_B\, T}{6\,\pi\,\eta\, r_A} \qquad (6)$$

where η is the viscosity of the solvent and r_A the radius of the corresponding solute A.

Once the apparent rate constants for all channels are obtained, reaction branching ratios can be estimated simply dividing by the overall rate constant. The branching ratios provide clues about the dominant mechanisms operating in the antioxidant process.

Results and discussion

We have studied the radical scavenging activity of TRA in aqueous media. Two different radicals of biological relevance have been selected, namely hydroxyl ($HO^\bullet$) and hydroperoxyl ($HOO^\bullet$). In both cases, we have considered different possible mechanisms for the reaction of TRA with a radical (R•):

- Radical adduct formation (RAF) $TRA + R^\bullet \rightarrow [TRA\text{-}R]^\bullet$
- Hydrogen atom transfer (HAT) $TRA + R^\bullet \rightarrow [TRA(-H)]^\bullet + RH$
- Single electron transfer (SET) $TRA + R^\bullet \rightarrow [TRA^+]^\bullet + R^-$

Through all these mechanisms a new radical species (adduct, dehydrogenated or cationic TRA) is formed, but now the indole ring contributes to stabilize the unpaired electron and therefore to diminish drastically its reactivity.

Other mechanisms invoked in the literature are the proton coupled electron transfer (PCET) and sequential electron proton transfer (SEPT). In the PCET mechanism transfer of an electron takes place simultaneously to a proton transfer. The resulting products are the same as in the HAT mechanism, and an analysis of the transition state involved is required to distinguish between HAT and PCET mechanisms. In the SEPT mechanism the proton transfer occurs after the electron transfer, giving finally the same products as in the HAT mechanism. Since proton transfer is usually fast, the rate of the SEPT mechanism should be essentially controlled by the SET step.

A previous study[22] of the conformational space of TRA in aqueous media concluded that the most stable conformer is that represented in Figure 1. Therefore, we have adopted in our work this structure. The site numbering employed is also shown in Figure 1. Possible addition sites for the RAF mechanism are the carbon atoms in the indol, namely C1, C2, C3, C4, C5, C6, C7 and C8 according to our notation. For the HAT mechanism we may identify as possible reactive sites N1, N2, C9 and C10. Therefore, in principle, all centers of the molecule might be involved in the antioxidant activity.

The processes studied in the present work correspond to the reactions of TRA with the radicals $HO^\bullet$ and $HOO^\bullet$:

$TRA + HO^\bullet \rightarrow$ (Reaction 1)
$TRA + HOO^\bullet \rightarrow$ (Reaction 2)

The notation of the species involved in the different processes would refer to the mechanism (RAF, HAT, SET) followed by a number indicating the reaction (1 for $HO^{\bullet}$, 2 for $HOO^{\bullet}$), the nature of the species (PROD for a product, TS for a transition state), and finally the center of the molecule where the radical attack is taking place according to the notation shown in Figure 1. Finally, in some cases a letter would be added at the end of the notation: A indicating either the *top* part of the indole ring or the *right* side of the aminoethyl chain, and B denoting the *bottom* part of the ring or the *left* side of the chain (according to the schematic structure of TRA shown in Figure 1).

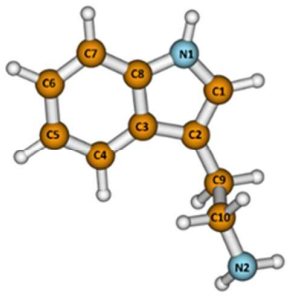

Figure 1. Schematic representation of the structure of TRA in aqueous solution with numbering of atoms employed in the present work.

Reaction of tryptamine with $HO^{\bullet}$

The structures of the products obtained in the reaction of tryptamine with $HO^{\bullet}$ through the RAF mechanism are shown in Figure 2, whereas those of the corresponding transition states are given in Figure 3. Relative energies and Gibbs free energies of the adducts and transition states are given in Table 1. RAF rate constants and apparent RAF rate constants, taking into account the diffusion process, for each reaction site are also given in Table 1. Following the suggestion of Galano and Alvarez-Idaboy,[30] to compute the diffusion rate constant R_{AB} is estimated as: a) the distance between the two atoms involved in the formation of the bond, taken form the transition state, for the RAF mechanism; b) the sum of the radius of both reactants (TRA and $HO^{\bullet}$) for the SET mechanism; c) the distance in the transition state between the two atoms involved in the hydrogen transfer for the HAT mechanism.

In all the formed adducts the hydrogen of the incoming $HO^{\bullet}$ radical points to the indole ring. The C-O distance for most adducts is very similar, taking values around 1.45-1.46 Å, except at C1 which is somewhat shorter (1.435 Å) and C3 with a longer value (1.485 Å).

There are no significant differences in the stability of the A and B RAF products. It seems that the attack through the *top* orientation (the same side as the aminoethyl chain) is slightly favored for the C5, C6, C7 and C8 centers, whereas the bottom orientation (opposite to the chain) is slightly preferred for the RAF products on C1, C2 and C3. This slight preference might be due to steric repulsion of the incoming $HO^{\bullet}$ radical with the chain.

The indole ring remains nearly planar in all adducts, except for those resulting from addition at C3 and C8, the two carbon atoms connecting the phenyl and pyrrole rings. The ∠C4C3C8N1 dihedral angle for these adducts is around 155 degrees, reflecting the deviation from planarity of the indole ring. This important distortion of the geometry, associated to a large extent to the loss of aromaticity, has direct consequences in the stability of the corresponding adducts. The C3 and C8 adducts are less stable than the rest of addition products, as can be seen in Table 1. In fact, addition at C3 is endergonic by more than 3 kcal/mol, whereas addition at C8 is only slightly exergonic.

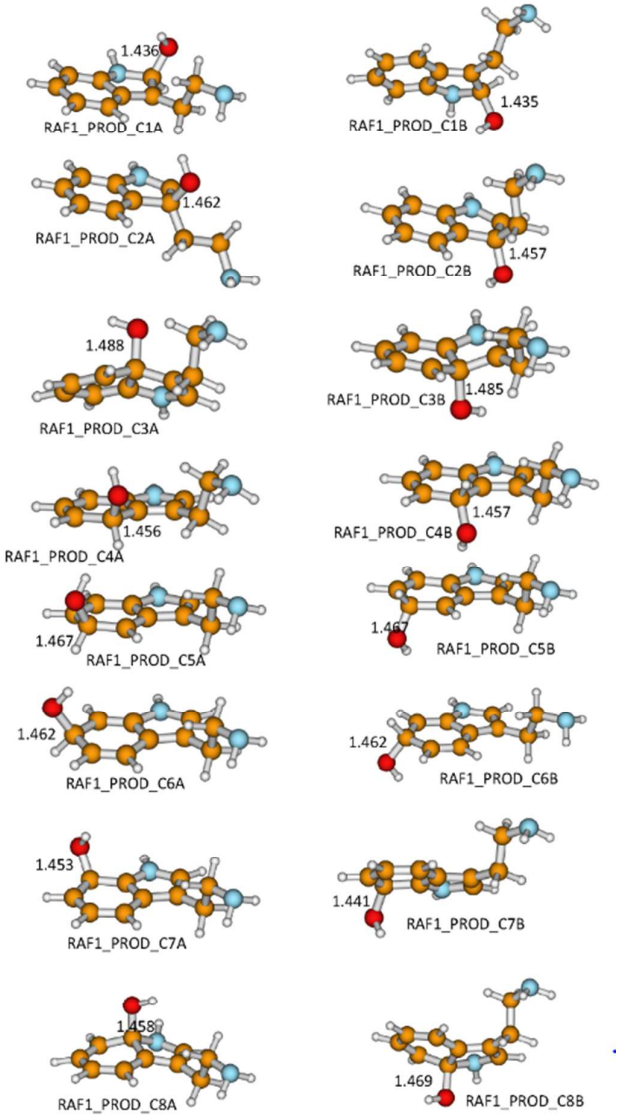

Figure 2. Optimized geometries of the products corresponding to the RAF mechanism of the TRA + HO$^{\bullet}$ reaction. Distances are given in Å.

In agreement with these results, when the Molecular Electrostatic Potential (MEP) was analyzed, diminished reactivity at C3 and C8 to the electrophilic attack was shown.[22] The rest of addition channels are thermodynamically favored as illustrated by their negative Gibbs free energy. The most exergonic RAF channel is addition at C1, the carbon atom belonging exclusively to the pyrrole ring and closest to N1. This outcome is also supported by the behavior of MEPs, which showed the highest reactivity of the indole ring to electrophilic attack close to C1.[22] This addition seems to be so favorable that no transition state for this process was characterized. We found the corresponding transition state in the gas phase. However all our attempts to obtain this TS in aqueous solution failed. Relaxed scans, following the C-O distance and optimizing all other geometrical variables, showed no sign of a barrier in aqueous solution, and as the oxygen atom approaches C1 the energy lowers reaching the adduct.

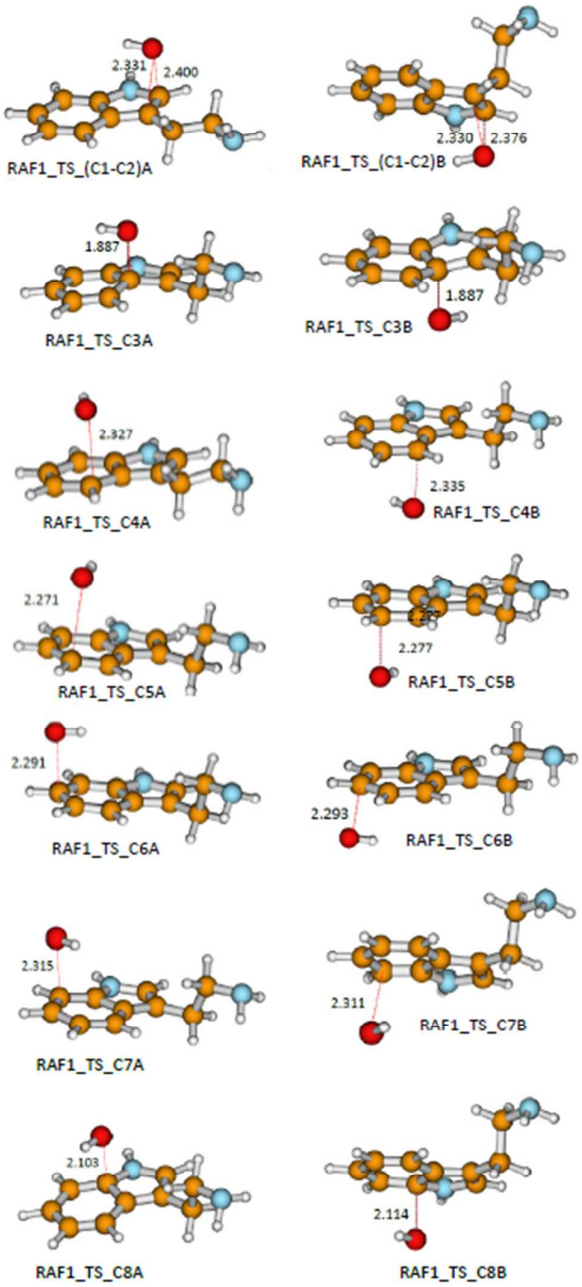

Figure 3. Optimized geometries of the transition states corresponding to the RAF mechanism of the TRA + HO$^{\bullet}$ reaction. Distances are given in Å.

Table 1. Relative Gibbs free energies (including thermal correction energies at 298 K) of the products (ΔG) and transition states ($\Delta G^{\neq}$), imaginary frequencies (ν, cm^{-1}) of the transition states, RAF rate constants (k^{RAF}), diffusion constants (k_D) and apparent RAF rate constants (k_{app}^{RAF}) for the RAF mechanism in the reactions of tryptamine with HO•. All energies are given in kcal/mol and rate constants in M^{-1} s^{-1}.

path	ΔG	$\Delta G^{\neq}$	ν	k^{RAF}	k_D	k_{app}^{RAF}
C1A	-23.38	-3.19[a]	-	3.31×10^{16}	2.53×10^{9}	5.06×10^{9}
C1B	-24.22	-3.19[a]	-	3.31×10^{16}	2.53×10^{9}	5.06×10^{9}
C2A	-13.34	-0.43[b]	90i	-	-	-
C2B	-14.43	-1.55[b]	89i	-	-	-
C3A	3.82	9.03	395i	3.65×10^{7}	2.14×10^{9}	3.59×10^{7}
C3B	3.33	8.89	403i	4.63×10^{7}	2.14×10^{9}	4.53×10^{7}
C4A	-15.38	3.11	269i	7.98×10^{11}	2.64×10^{9}	2.63×10^{9}
C4B	-15.39	2.09	242i	4.46×10^{12}	2.65×10^{9}	2.65×10^{9}
C5A	-9.37	2.69	271i	1.62×10^{12}	2.58×10^{9}	2.58×10^{9}
C5B	-9.20	2.77	267i	1.42×10^{12}	2.59×10^{9}	2.58×10^{9}
C6A	-11.98	3.15	338i	7.46×10^{11}	2.60×10^{9}	2.59×10^{9}
C6B	-11.17	2.69	345i	1.62×10^{12}	2.61×10^{9}	2.60×10^{9}
C7A	-14.6	3.09	252i	8.25×10^{11}	2.62×10^{9}	2.62×10^{9}
C7B	-14.4	2.29	259i	3.18×10^{12}	2.63×10^{9}	2.62×10^{9}
C8A	-3.16	5.72	146i	9.75×10^{9}	2.39×10^{9}	1.92×10^{9}
C8B	-2.67	5.93	137i	6.84×10^{9}	2.40×10^{9}	1.78×10^{9}

[a]Estimated from a single-point calculation on the gas-phase structure of the transition state.

[b]Relative Gibbs free energy of the TS corresponding to the isomerization of the C2-C1 products.

The study of MEPs in the gas phase and in solution justifies this behavior. It was found a large increment in reactivity to electrophilic attack close to C1 when the system was modeled in aqueous solution by a Polarized Continuum Medium model.[22] Therefore, it seems that this process may proceed without an activation barrier in aqueous solution. Nevertheless, in Table 1 we provide the energy barrier resulting from a single-point calculation in aqueous solution at the geometry of the located TS in the gas phase. The activation Gibbs free energy is -3.19 kcal/mol, thus confirming the hypothesis of a barrier-free process. The estimation of the rate constant employing this value should be taken just as an approximate value. However, since it takes a very high value, has no practical consequence, since the corresponding C1 RAF channel should be diffusion-controlled.

Another peculiar case is the RAF channel for C2. This is a clearly exergonic process as well, but we were not able to obtain a transition structure neither in aqueous solution nor in the gas phase. In this case, all our attempts to characterize the transition states led to the transition structures corresponding to the migration of the incoming HO• radical from C2 to C1. These are the structures termed RAF1_TS_(C1-C2)A/B in Figure 3. Their Gibbs free energy (after taking into account the corrections in solution) are -0.43 and -1.55 kcal/mol, respectively for the A (top) and B (bottom) transition states. It seems that as soon as the HO• radical approaches C2, formation of the C1 adduct is so favorable that the HO• radical migrates to C1. Again, the study of MEPs gives support to these features; in fact, the negative values of MEP which allowed to describe sites of electrophilic attack, showed that C1 is close to a site which is more reactive than C2 site by approximately 70%.[22] Therefore, we may conclude that the RAF channel starting at C2 would lead in fact to the barrierless formation of C1. Consequently, we must count twice the contribution of the C1 RAF channel.

We were able to characterize the transition states in aqueous solution for the rest of RAF channels C3-C8 (imaginary frequencies of the transition states are included in Table 1). In all cases the C-O distances are in the range 2.1-2.3 Å, with the exception of TS_C3A/B which have a shorter distance (1.887 Å). For C4, C5, C6 and C7 energy barriers of 2-3 kcal/molare found, whereas the less favorable channels at C3 and C8 have noticeable larger barriers. In fact, as Galano and Alvarez-Idaboy[30] suggest, it is unnecessary to calculate the energy barrier for the C3 RAF channel, since this is an endergonic process. Even if the endergonic path takes place at a significant rate, it would be reversible and the formed products will not be observed.[30] In the present case, a formal evaluation of the rate constant for the C3 RAF channel shows a rather low value, two orders of magnitude lower than the diffusion limit, leading to the conclusion that this channel should not be effectively observed. In what follows we will omit the calculation of energy barriers for endergonic processes. As can be seen in Table 1, all remaining RAF channels have similar apparent rate constant, since they are mainly diffusion- controlled, except that involving C8 which is somewhat lower due to the larger barrier found in this case. The most favorable center seems to be C1, with rate constants which nearly double the rest of

centers for the RAF mechanism. All these results are also in agreement with the characteristics of MEPs mentioned above which were described in a previous work.[22]

Table 2. Vertical energy difference (ΔE), Gibbs free energy of reaction (ΔG^o), reorganization energy (λ), Gibbs free energy of activation ($\Delta G^{\neq}$), SET rate constant (k^{SET}), and apparent SET rate constant (k_{app}^{SET}) for the SET mechanism in the reactions of tryptamine with HO$^\bullet$ and HOO$^\bullet$. All energies are given in kcal/mol and rate constants in M^{-1} s^{-1}.

	ΔE	ΔG^o	λ	$\Delta G^{\neq}$	k^{SET}	k_{app}^{SET}
TRA + HO$^\bullet$	1.58	-6.14	7.72	0.08	1.32×10^{14}	8.19×10^{9}
TRA + HOO$^\bullet$	36.56	16.91	19.65	17.01	51.67	51.67

The different parameters (vertical energy difference, Gibbs free energy of reaction, and reorganization energy) required to estimate the SET rate constant are given in Table 2. As can be seen, the Gibbs free energy of the reaction is negative and therefore the process is thermodynamically viable. The resultant activation barrier for this process is very small, leading to a very high electron transfer rate constant. The consequence is that the process is diffusion-controlled, with an apparent rate constant higher than any individual RAF channel.

Finally, the corresponding data for the HAT mechanism are collected in Table 3, whereas the structures of the products and transition states involved in the HAT mechanism for the reaction of TRA with HO$^\bullet$ are provided in Figures 4 and 5, respectively. The main changes found in the optimized geometries of HAT products, shown in Figure 4, are related to the aminoethyl chain, whereas the indole ring remains planar. As can be seen in Table 3 all channels are clearly exergonic, showing that all these processes are thermodynamically favored compared to the RAF and SET mechanisms. It seems that hydrogen transfer from C9 and N1 are the most favorable sites for the HAT mechanism. Furthermore, it is noticeable that the HAT apparent rate constants in TRA are for N1 one order of magnitude higher than in MLT, and for C9 two orders of magnitude higher than in MLT.[10] These findings reveal the effect of substituents. We hope that subsequent studies of electronic distribution will allow us to understand these TRA-MLT variations. These results can be related to the highest positive values of MEP at hydrogen atom attached to N1, and the high positive value at hydrogen atom B bonded to C9, as previously found.[22] For N1 we were only able to characterize the transition state in the gas phase, since all our attempts in solution failed. Again, the study of MEPs in the gas phase and their changes in solution could explain these results because an augmented reactivity for nucleophilic attack (about 40%) at hydrogen bonded to N1 was observed when it was considered in the aqueous solvent.[22] A single-point calculation in solution at the gas-phase geometry provided a value of -1.65 kcal/mol for $\Delta G^{\neq}$, suggesting quite likely that in fact there will be no transition state in solution and the rate constant should be the corresponding diffusion constant.

For the rest of HAT sites we have estimated the rate constant taking into account the correction for tunneling. Nevertheless, as can be seen in Table 3, the tunneling coefficients in all cases are rather low, within the range 1-2, mainly as a consequence of the relatively low imaginary frequency associated to the transfer of the hydrogen atom. In any case, the HAT rate constants are at least one order of magnitude higher than the diffusion constants, and the apparent rate constants in all cases are close to the diffusion constants. There seems to be no significant differences in the individual rate constants for each path, and all reaction sites should contribute in a rather similar proportion.

Table 3. Relative Gibbs free energies (including thermal correction energies at 298 K) of the products (ΔG) and transition states ($\Delta G^{\neq}$), imaginary frequencies (ν, cm^{-1}) of the transition states, tunnelling coefficients (κ), HAT rate constants (k^{HAT}), diffusion constants (k_D) and apparent HAT rate constants (k_{app}^{HAT}) for the HAT mechanism in the reactions of tryptamine with HO$^\bullet$. All energies are given in kcal/mol and rate constants in M^{-1} s^{-1}.

path	ΔG	$\Delta G^{\neq}$	ν	κ	k^{HAT}	k_D	k_{app}^{HAT}
N1	-35.02	-1.95[a]	-	-	4.08×10^{15}	2.96×10^{9}	2.96×10^{9}
C9A	-37.01	1.87	438 i	1.21	7.82×10^{12}	3.25×10^{9}	3.25×10^{9}
C9B	-35.33	5.25	784 i	1.91	2.16×10^{10}	3.11×10^{9}	2.89×10^{9}
C10A	-32.29	4.17	666 i	1.58	1.33×10^{11}	3.11×10^{9}	3.06×10^{9}
C10B	-31.63	4.71	628 i	1.50	5.36×10^{10}	3.13×10^{9}	3.01×10^{9}
N2A	-26.16	5.69	657 i	1.57	1.02×10^{10}	2.92×10^{9}	2.47×10^{9}
N2B	-26.96	5.42	640 i	1.53	1.62×10^{10}	2.64×10^{9}	2.38×10^{9}

[a]Estimated from a single-point calculation on the gas-phase structure of the transition state.

.

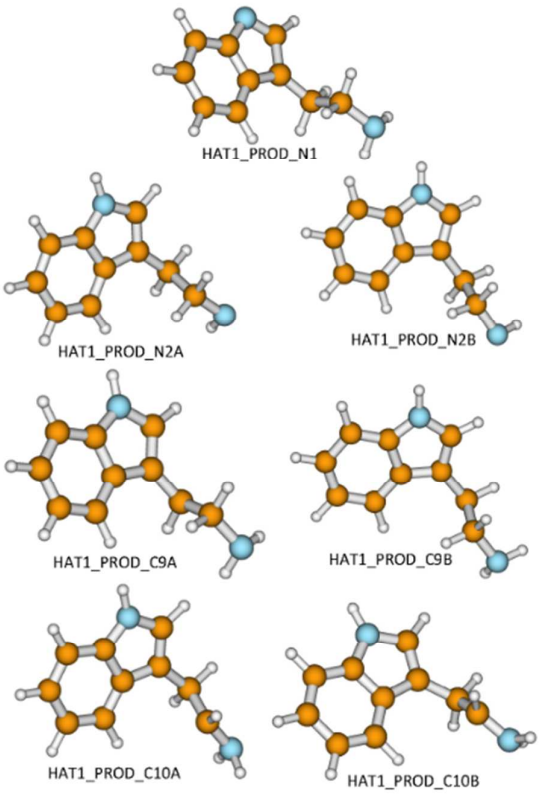

Figure 4. Optimized geometries of the products corresponding to the HAT mechanism of the TRA + HO$^{\bullet}$ and TRA + HOO$^{\bullet}$ reactions

Once all individual rate constants have been obtained, we can compute the global rate constants for each mechanism just summing up the contribution of each individual channel. The overall rate constant is then computed as:

$$k^{overall}=k^{RAF} + k^{SET} + k^{HAT} \qquad (7)$$

In Table 4 we summarize the results for the reaction of TRA with HO$^{\bullet}$ in water at 298 K, along with the corresponding branching ratios for each mechanism.

Table 4. Global apparent rate constants (M^{-1} s^{-1}), including diffusion correction, and direct branching rations at 298 K for the three considered mechanisms in the reaction of tryptamine with HO$^{\bullet}$.

Path	k_{app}	Γ (%)
RAF	3.47 x 10^{10}	55.16
SET	8.19 x 10^{9}	13.02
HAT	2.00 x 10^{10}	31.82

It seems that RAF should be the dominant mechanism, accounting for more than the half of the reaction, followed by the HAT mechanism with approximately a third part of the products. Finally, the less contributing mechanism is SET, with a branching ratio of 13%. Nevertheless, this value is of the same magnitude than the branching ratio for the most contributing site in the RAF

mechanism, namely C1. The sum of the branching ratios for the C1A and C1B channels in the RAF mechanism is 16.10%, only slightly higher than the branching ratio for the SET mechanism. The overall rate constant is relatively high, namely 6.29 x 10^{10} M^{-1} s^{-1}, suggesting that tryptamine is an efficient scavenger for HO• radicals in water.

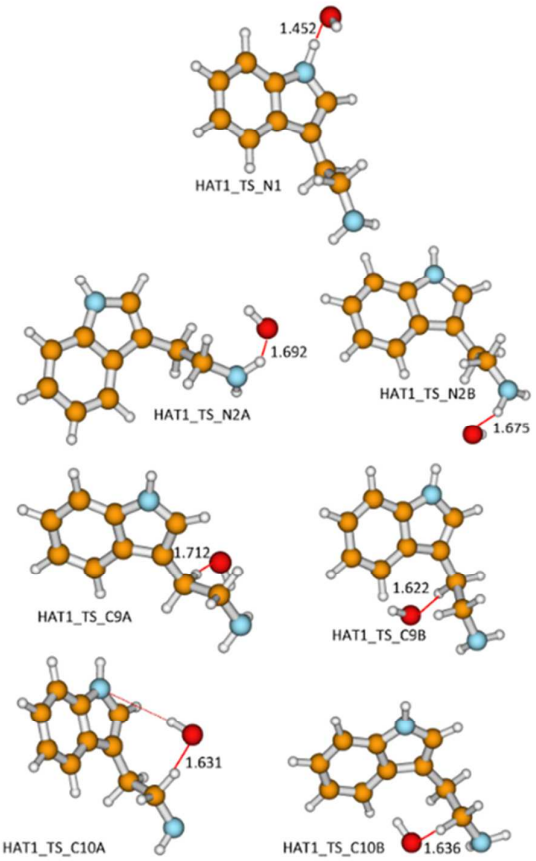

Figure 5. Optimized geometries of the transition states corresponding to the HAT mechanism of the TRA + HO• reaction. Distances are given in Å.

Reaction of tryptamine with HOO•

We now consider the reaction of TRA with HOO• taking into account the same mechanisms as in the preceding section.

The relative reaction energies (including ZPE corrections) and the Gibbs free energies (including thermal corrections at 298 K) of the products for the RAF mechanism are given in Table 5, the corresponding optimized geometries are given as supplementary information in Figure S1. It can be readily seen that, even though the paths C1A and C1B are exothermic, finally all paths are endergonic. Therefore, the RAF mechanism does not seem viable for the reaction of TRA with HOO• because, as mentioned before, the fact that all paths are endergonic means that, even if the products could be formed, they would evolve toward the reactants given the reversibility of the process. Consequently, the RAF channel should be ruled out as a possible mechanism for this reaction. The different behavior observed between the HO• and HOO• radicals could be related to their respective electron-accepting character, as suggested by Iuga et al.[27]

The corresponding parameters required to estimate the reaction constant for the SET mechanism of the reaction of TRA with HOO• are shown in Table 2. It can be readily seen that SET is also clearly endergonic and therefore this anticipates that this mechanism should be ruled out. Nevertheless, we have computed the rate constant, obtaining a value of 51.67 $M^{-1}s^{-1}$, which is consistent with a non-important path. In fact, when compared to the HAT mechanism (see below) the rate constant of the SET mechanism would lead formally to a branching ratio below 0.1%, thus confirming that its contribution should be in any case negligible for the present reaction. Analogous MLT studies led to similar results,[10] thus enlightening this behavior as intrinsic to aminoindole structures.

Table 5. Relative energies, including ZPE corrections, (ΔE) and Gibbs free energies, including thermal correction energies at 298 K (ΔG) of the products for the RAF mechanism in the reactions of tryptamine with HOO•. All energies are given in kcal/mol.

Path	ΔE	ΔG
C1A	-5.52	3.06
C1B	-5.97	2.48
C2A	4.91	13.35
C2B	3.87	12.32
C3A	19.86	28.83
C3B	22.04	30.74
C4A	0.63	9.43
C4B	1.22	9.75
C5A	7.64	16.01
C5B	7.71	16.09
C6A	5.23	13.45
C6B	5.44	13.96
C7A	2.47	10.52
C7B	2.93	11.49
C6A	14.04	22.92
C8B	14.33	23.12

Finally, the relevant data in the HAT mechanism are collected in Table 6. As can be seen only three paths are exergonic, namely N1, C9A and C9B.Therefore the sites C10 and N2 should not have any role in the HAT mechanism for the reaction between TRA and HOO•. In MLT instead, the exergonic processes correspond to C9 and C1 channels.[10] The changes MLT-TRA for N1 and C1 are again interesting substituent effects. The transition states for the exergonic paths are shown in Figure 6. It can be seen that the O-H distances in the transition states are much shorter than those found in the corresponding transition states of the reaction with HO•. This is probably related to the much higher imaginary frequencies observed in the case of the reaction with HOO• (see Tables 3 and 6).

Table 6. Relative Gibbs free energies (including thermal correction energies at 298 K) of the products (ΔG) and transition states ($\Delta G^{\neq}$), imaginary frequencies (ν, cm^{-1}) of the transition states, tunnelling coefficients (κ), HAT rate constants (k^{HAT}), diffusion constants (k_D) and apparent HAT rate constants (k_{app}^{HAT}) and branching ratios for the HAT mechanism in the reactions of tryptamine with HOO•. All energies are given in kcal/mol and rate constants in M^{-1} s^{-1}.

path	ΔG	$\Delta G^{\neq}$	ν	κ	k^{HAT}	k_D	k_{app}^{HAT}	Γ (%)
N1	-1.80	15.70[a]	2392 i	72.17	3.40×10^4	2.56×10^{10}	3.70×10^4	91.82
C9A	-3.79	16.02	1369 i	10.20	2.80×10^3	2.74×10^{10}	2.80×10^3	7.56
C9B	-2.11	17.47	1389 i	9.68	3.30×10^2	2.74×10^{10}	2.30×10^2	0.62
C10A	0.94	-						
C10B	1.59	-						
N2A	7.06	-						
N2B	6.27	-						

[a]Estimated from a single-point calculation on the gas-phase structure of the transition state.

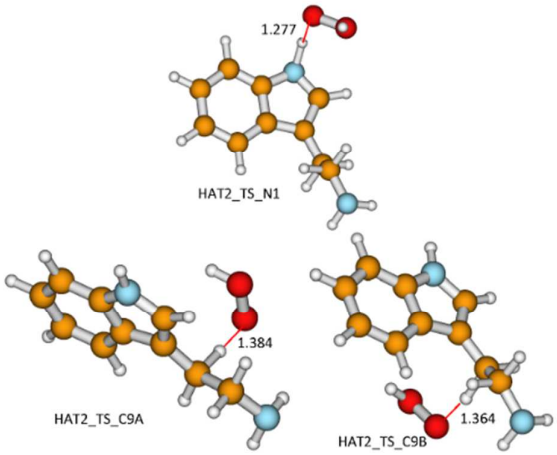

Figure 6. Optimized geometries of the transition states corresponding to the HAT mechanism of the TRA + HOO• reaction. Distances are given in Å.

The relatively high imaginary frequencies shown in Table 6 lead also to higher tunneling coefficients than in the case of the reaction with HO•. Nevertheless, the relative Gibbs free energies of the transition states are also much higher for the reaction with HOO•, leading finally to much smaller HAT rate constants. We have computed the diffusion constants as well, but it can be seen in Table 6 that in this case diffusion does not play any significant role, and the bottleneck for this reaction is the barrier of the transition state. The branching ratios, included in Table 6, suggest that more than 90% of the reaction should take place through the N1 site, with a minor role for C9. C10 and N2 should not play any role in this reaction.

The overall rate constant for the reaction of TRA with HOO• in water at 298 K takes a value of 3.71 x 10^4 M^{-1} s^{-1}, and corresponds entirely to the HAT channel, since both RAF and SET channels are endergonic. This a relatively fast value, compared to other processes in biological environments. For example, as discussed by Iuga et al[27] and de Grey,[42] the damage to unsaturated fatty acids caused by HOO• radicals takes place at rates around 1.18-3.05 x 10^3 M^{-1} s^{-1}, smaller than the scavenging activity of TRA toward HOO• radicals. It seems that TRA could act as a relatively efficient antioxidant.

Moreover, our results show that the behavior of TRA against radical HOO• is similar to that already reported for MLT, with the only exception of the changes found between MLT and TRA for N1 and C1 in the HAT mechanism.[10] This finding leads us to propose that the low reactivity towards said radical would be associated mainly with the indole heterocycle, being practically independent of the acetamidoethyl side chain and the methoxy group at site 5.

Finally, it is interesting to note that the overall rate constant of hydroxyl radical reaction (6.29 × 1010 M-1 s-1), is much higher than that of hydroperoxyl radical (3.71 × 104 M-1 s-1), and that recent experimental developments confirm this result.[43]

Conclusions

A computational kinetics evaluation of the antioxidant activity of tryptamine in water at 298 K has been carried out. Two different radicals have been considered, namely HO• and HOO•.

In the case of the hydroxyl radical nearly all channels are diffusion controlled. The overall rate constant is very high, 6.29 x 10^{10} M^{-1} s^{-1}, suggesting that tryptamine should react very rapidly with hydroxyl radicals. The dominant mechanism is RAF, with a branching ratio of 55%, followed by the HAT mechanism (31%) and finally SET (13%). The most favorable site for the RAF mechanism seems to be C1, the less hindered carbon atom neighbor to the nitrogen of the indole ring, accounting for 16% of the products. For the HAT mechanism no significant differences are found between the different possible centers participating in the mechanism.

The overall rate constant found for the reaction of tryptamine with the HOO• radical is much smaller, namely 3.71 x 10^4 M^{-1} s^{-1}, but still high enough as to be a competitive process with other reactions of hydroperoxyl radicals in biological environments. This may suggest that tryptamine could have a noticeable scavenging activity toward radicals. For the reaction with hydroperoxyl radicals the all RAF and the SET mechanisms are found to be endergonic, and the only viable mechanism is HAT. Furthermore, only two centers may contribute to the HAT mechanism, N1 and C9, the former accounting for more than 91% of the total products. Therefore, we may conclude that most of the antioxidant activity of tryptamine toward HOO• radicals comes from the nitrogen atom of the indole ring through hydrogen atom transfer, with a very minor contribution of the aminoethyl chain.

It draws the attention that HAT mechanism for the reaction between MLT and HOO• was reported as endergonic channel through N1 and exergonic channel from site C1.[10] In view of recent electronic studies[23] it is of our interest to study with the same detail the kinetics of SER, to analyze for example the change in the reactivity of N1 in TRA, as well as their high values of k_{app} for

the HAT channels from N1 and C9. In addition, a systematic comparison between in polar and nonpolar solvents and gas phase rate constants of radical reaction and their corresponding transition states at different sites would be significant for further kinetic study of TRA and other indole antioxidants.

Conflicts of interest

There are no conflicts to declare.

Supporting Information

Optimized geometries of the products corresponding to the RAF mechanism of the TRA + OOH reaction. Cartesian coordinates of the transition states.

Acknowledgements

E.N.B. acknowledges a fellowship of CONICET (Argentina), and Universidad Nacional del Nordeste (Corrientes, Argentina). R.M.L. acknowledges Centro de Cómputos de Alto Desempeño de la Universidad Nacional del Nordeste (CADUNNE) for computing facilities, and financial support of the Secretaria General de Ciencia y Técnica de la Universidad Nacional del Nordeste (Corrientes, Argentina) (Grant F008-2013), H.M, P.R. and A.L. acknowledge financial support from the Spanish Ministerio de Economía Industria y Competitividad (Grant AYA2017-87515-P).

References

1 Cotelle, J. L.; Bernier, J. L.; Catteau, J. P.; Pommery, J.; Wallet, J. C.; Gaydou, E. M. Antioxidant Properties of Hydroxy-flavones. *Free Radic. Biol. Med.* **1996,** *20,* 35-46.

2 Kruk, I.; Aboul-Enein, H. Y.; Michalska, T.; Lichszteld, K.; Kubasik-Kladna, K; Olgen, S. In Vitro Scavenging Activity for Reactive Oxygen Species by N-substituted Indole-2-carboxylic Acid Esters. *J. Lumin.* **2007,** *22*, 379-386.

3 Shirinzadeh, H.; Eren, B.; Gurer-Orhan, H.; Suzen, S.; Ozden, S. Novel Indole-based Analogs of Melatonin: Synthesis and In Vitro Antioxidant Activity Studies. *Molecules* **2010,** *15*, 2187-2202.

4 Tan, D. X.; Chen, L. D.; Poeggeler, B.; Manchester, L. C.; Reite, R. J. Melatonin: A Potent, Endogenous Hydroxyl Radical Scavenge. *Endocr. J.* **1993,** *1*, 57-60.

5 Melchiorri, D.; Reiter, R. J.; Attia, A. M.; Hara, M.; Burgos, A.; Nistico, G. Potent Protective Effect of Melatonin on In Vivo Paraquat-induced Oxidative Damage in Rats. *Life Sci.* **1994,** *56*, 83-89.

6 Matuszak, Z.; Reszka, K. J.; Chignell, C. F. Reaction of Melatonin and Related Indoles With Hydroxyl Radicals: EPR and Spin Trapping Investigations. *Free Radical Biol. Med.* **1997,** *23*, 367-372.

7 Sofic, E.; Rimpapa, Z.; Kundurovic, Z.; Sapcanin, A.; Tahirovic, I.; Rustembegovic, A.; Cao, G. J. Antioxidant Capacity of the Neurohormone Melatonin. *Neural Transm.* **2005**, *112*, 349-358.

8 Tujanski, A. G.; Rosenstein, R. E.; Estrin, D. A. Reactions of Melatonin and Related Indoles with Free Radicals: A Computational Study. *J. Med. Chem.* **1998,** *41,* 3684-3689.

9 Stasica, P.; Paneth, P.; Rosiak, J. M.; Hydroxyl Radical Reaction with Melatonin Molecule: A Computational Study. *J. Pineal Res.* **2000,** *29*, 125-127.

10 Galano, A. On the Direct Scavenging Activity of Melatonintowards Hydroxyl and a Series of Peroxyl Radicals. *Phys. Chem. Chem. Phys.* **2011,** *13*, 7178-7188.

11 Galano, A.; Tan, D. X.; Reiter, R. J. On the Free Radical Scavenging Activities of Melatonin's Metabolites, AFMK and AMK. *J. Pineal Res.* **2013,** *54*, 245-257.

12 Alvarez-Didak, R.; Galano, A.; Tan, D. X.; Reiter, R. J. Álvarez-Didak, R.; Galano, A.; Tan, D. X.; Reiter, R. J. N-Acetylserotonin and 6-Hydroxymelatonin Against Oxidative Stress: Implications for the Overall Protection Exerted by Melatonin. *J. Phys. Chem. B* **2015**, *119*, 8535-8543.

13 Galano, A. Computational-aided Design of Melatonin Analogues with Outstanding Multifunctional Antioxidant Capacity. *Roy. Soc. Chem. Adv.* **2016,** *6*, 22951-22963.

14 Gozzo, A.; Lesieur, D.; Duriez, P.; Fruchart, J. C.; Teissier, E. Structure-activity Relationships in a Series of Melatonin Analogues with the Low-density Lipoprotein Oxidation Model. *Free Radical Biology and Medicine* **1999,** *26*, 1538-1543.

15 Poeggeler, B.; Thuermann, S.; Dose, A.; Schoenke, M.; Burkhardt, S.; Hardeland, R., Melatonin's Unique Radical Scavenging Properties – Roles of its Functional Substituents as Revealed by a Comparison with its Structural Analogs. *J. Pineal Res.* **2002,** *33*, 20–30.

16 Phillips, L. A.; Levy, D. H., Rotationally Resolved Electronic Spectroscopy of Tryptamine Conformers in a Supersonic Jet. *J. Chem. Phys.* **1988,** *89*, 85-90.

17 Carney, J. R.; Zwier, T. S. The Infrared and Ultraviolet Spectra of Individual Conformational Isomers of Biomolecules: Tryptamine. *J. Phys. Chem. A* **2000,** *104*, 8677-8688.

18 Clarkson, J. R.; Dian, B. C.; Moriggi, L.; DeFusco, A.; McCarthy, V.; Jordan, K. D.; Zwier, T. S. Direct Measurement of the Energy Thresholds to Conformational Isomerization in Tryptamine: Experiment and Theory. *J. Chem. Phys.* **2005,** *122*, 214311-1 – 214311-15.

19 Böhm, M.; Brause, R.; Jacoby, C.; Schmitt, M. Conformational Relaxation Paths in Tryptamine *J. Phys. Chem. A* **2009,** *113*, 448-455.

20 Marochkin, I. I.; Altova, E. P.; Rykov, A. N.; Shishkov. I. F. Molecular Structure of Tryptamine in Gas Phase According to Gas Electron Diffraction Method and Quantum Chemistry Calculations. *J. Mol. Struct.* **2017,** *1148*, 179-184.
21 Lobayan, R. M.; Pérez Schmit, M. C.; Jubert, A. H.; Vitale, A. Conformational and Stereoelectronic Investigation of Tryptamine. An AIM/NBO Study. *J. Mol. Model.* **2012,** *18*, 2577-2588.
22 Lobayan, R. M.; Pérez Schmit, M. C.; Jubert, A. H.; Vitale, A Aqueous Solvent Effects on the Conformational Space of Tryptamine. Structural and Electronic Analysis. *J. Mol. Model.* **2013,** *19*, 1109-1123.
23 Lobayan, R. M.; Pérez Schmit, M. C. Conformational and NBO Studies of Serotonin as a Radical Scavenger.Changes Induced by the OH. *J. Mol. Graph. Model.* **2018,** *80*, 224–237.
24 Pryor, W. A. Oxy-radicals and Related Species: their Formation, Lifetimes, and Reactions. *Annu. Rev. Physiol.* **1986,** *48*, 657-667.
25 Galano, A.; Francisco-Marquez, M.; Alvarez-Idaboy, J. R. Mechanism and Kinetics Studies on the Antioxidant Activity of Sinapinic Acid. *Phys. Chem. Chem. Phys.* **2011,** *13*, 11199-11205.
26 Galano, A. Mechanism and Kinetics of the Hydroxyl and Hydroperoxyl Radical Scavenging Activity of N-acetylcysteine Amide. *Theor. Chem. Acc.* **2011,** *130*, 51-60.
27 Iuga, C.; Alvarez-Idaboy J. R.; Russo, N. Antioxidant Activity of Trans-Resveratrol toward Hydroxyl and Hydroperoxyl Radicals: A Quantum Chemical and Computational Kinetics Study. *J. Org. Chem.* **2012,** *77*, 3868-3877.
28 Leon-Carmona, J. R; Galano, A., Free Radical Scavenging Activity of Caffeine's Metabolites. *Int. J. Quantum Chem.* **2012,** *112*, 3472-3478.
29 Villuendas-Rey, Y.; lvarez-Idaboy, J. R.; Galano, A., Assessing the Protective Activity of a Recently Discovered Phenolic Compound Against Oxidative Stress using Computational Chemistry. *J. Chem. Inf. Model.* **2015,** *55*, 2552-2561.
30 Galano, A.; Alvarez-Idaboy, J. R. A Computational Methodology for Accurate Predictions of Rate Constants in Solution: Application to the Assessment of Primary Antioxidant Activity. *J. Comput. Chem.* **2013,** *34*, 2430-2445.
31 Zhao, Y.; Schultz, N. E.; Truhlar, D. G. A Design of Density Functionals by Combining the Method of Constraint Satisfaction with Parametrization for Thermochemistry, Thermochemical Kinetics, and Noncovalent Interactions. *J. Chem. Theory Comput.* **2006**, *2*, 364-382.
32 Krishnan, R.; Binkley, J.S.; Seeger, R.; Pople, J. A. Self-consistent Molecular Orbital Methods. XX. A Basis Set for Correlated Wave Functions. *J. Chem. Phys.* **1980,** *72*, 650-654.
33 Frisch M.J.; Trucks G.W.; Schlegel H.B.; Scuseria G.E.; Robb M.A.; Cheeseman, G. W.; Scalmani, G.; Barone, V.; Mennucci, B.; Petersson, G. A., et al. *Gaussian 09*, Revision B.01, Inc.: Wallingford, CT, 2010.
34 Marenich, A. V.; Cramer, C. J.; Truhlar, D. G. Universal Solvation Model Based on Solute Electron Density and on a Continuum Model of the Solvent Defined by the Bulk Dielectric Constant and Atomic Surface. *J. Phys. Chem.* B **2009,** *113*, 6378-6396.
35 Okuno, Y. Theoretical Investigation of the Mechanism of the Baeyer-Villiger Reaction in Nonpolar Solvents. *Chem. Eur. J.* **1997,** *3*, 212-218.
36 Truhlar, D. G.; Isaacson, A. D.; Skodje, R. T.; Garrett, B. C. Incorporation of Quantum Effects in Generalized-transition-state Theory. *J. Phys. Chem.* **1982,** *86*, 2252-2261.
37 Marcus, R. A. Annu. Chemical and Electrochemical Electron-transfer Theory. *Rev. Phys. Chem.* **1964,** *16*, 155-196.
38 Marcus, R. A., Electron Transfer Reactions in Chemistry. Theory and Experiment. *Rev. Mod. Phys.* **1993,** *65*, 599-610.
39 Nelsen, S. F.; Blackstock, S. C.; Kim Y., Estimation of Inner Shell Marcus Terms for Amino Nitrogen Compounds by Molecular Orbital Calculations. *J. Am. Chem. Soc.* **1987,** *109*, 677-682.
40 Nelsen, S. F.; Weaver, M. N.; Luo, Y.; Pladziewicz, J. R.; Ausman, L. K.; Jentzsch, T. L.; Knek, J. J., Estimation of Electronic Coupling for Intermolecular Electron Transfer from Cross-reaction Data. *J. Phys. Chem. A* **2006,** *110*, 11665-11676.
41 Truhlar, D. G., Nearly Encounter-controlled Reactions: The Equivalence of the Steady-state and Diffusional Viewpoints. *J. Chem. Educ.* **1985,** *62*, 104-106.
42 de Grey, A. D. N. J., HO2•: The Forgotten Radical. *DNA Cell Biol.* **2002,** *21*, 251-257.
43 Zhao H., Wang Q., Chen Y., Tian Q., Zhao G., Efficient removal of dimethyl phthalate with activated iron-doped carbon aerogel through an integrated adsorption and electro-Fenton oxidation process. *Carbon* **2017**, 124, 111-122.

TOC Graphic

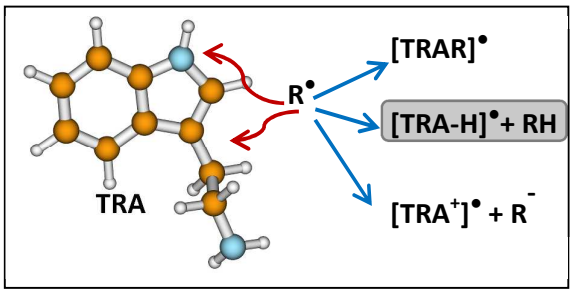

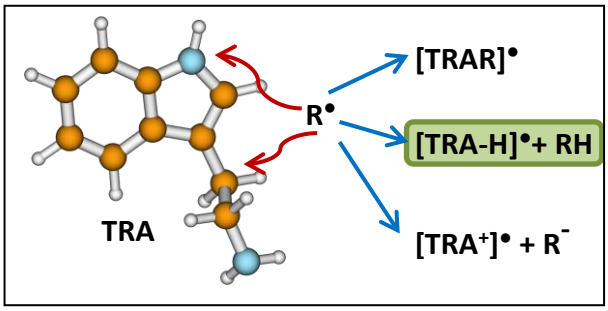
[TRAR]•
R•
[TRA-H]•+ RH
TRA
[TRA+]• + R-